IOP Conf. Series: Materials Science and Engineering **400** (2018) 022057 doi:10.1088/1757-899X/400/2/022057

Aspects regarding the contact between wheels and turnouts

C Tudorache, R Oprea and M Stafie
University Politehnica of Bucharest- Romania, Faculty of Transportation, Railway Vehicles Engineering Department, Splaiul Independentei nr. 313, Sector 6, Bucuresti, CP 060042

E-mail: cristi_tudorache2003@yahoo.com, razvan.oprea@gmail.com

Abstract. Wheel and turnouts life safe operation and life span prediction may be improved through a more thorough research. Currently, numerical methods for the study of the before mentioned problem bring significant overhead in computing systems. The present work describes a multi-point contact study between wheel and switch using Kalker's three-dimensional theory, using CONTACT software. This method has the advantage to suit well the frictional aspects of the phenomena. More than that, comparisons between results obtained with FE software and with CONTACT software reveal a remarkable similarity. The latter method however, is significantly more efficient from the numerical method point of view and it also allows computing the contact points position either on the fly or using look up tables.

1. Introduction

Developing computer applications for the study of train–turnout interaction has been a main goal in the recent years for both the UIC (International Union of Railways) and railway researchers [1]. The subjet has been approached employing commercial multi-body or finite element (FE) software. In the proposed methods contact points position is computed either on the fly or using look-up tables.

In the case of the latter method, contact points coordinates are computed in advance, stored in look-up tables and intermediate points are determined using interpolation [2,3,4].

If the contact resolution is performed on the fly, iterations and secondary contact points search is necessary.

Whether the first or the second method is used, the computation brings significant overhead, even for powerful computation systems available today. Various methods to express constraint contact forces may be employed, e.g., Lagrange multipliers.

The present paper will employ Kalker's three dimensional theory in the research of the train–turnout interaction. This method has the advantage to suit well the frictional aspects of the phenomena. More than that, comparisons between results obtained with FE software and with CONTACT software reveal a remarkable similarity [5]. The latter method however, is significantly more efficient from the numerical method point of view and it also allows using any of the two contact points computation methods mentioned above.

The presence of of simultaneous contact points on wheels in contact with the turnout is an intrinsic feature of the phenomena. FE analysis is difficult to apply as contact areas depend on the deformation of the bodies and the deformations depend on the contact forces and areas.

IOP Conf. Series: Materials Science and Engineering **400** (2018) 022057 doi:10.1088/1757-899X/400/2/022057

2. Basic knowledge of Kalker's theory

The tangential force dependence on creep in rolling contacts features a maximum, known as friction saturation. Starting from a null value, the gradual increase of the creepage leads to the friction saturation. Further, creepage amplifying is followed by a decreasing force section.

During the past decades a number of wheel-rail contact theories have been developed, based on Kalker's research. The studies aim is to define the relationship between forces, spin moment and linear and spin creepage. Each model has its limitation therefore several theories were introduced [29], i.e., linear theory, strip theory, empirical theory, simplified theory and exact three dimensional rolling contact theory.

The linear theory may handle small spin and creepages. This assumption neglects the pressure applied at the edges of the contact area. Hence, the boundary conditions are not enforced at the trailing edge where the wheel and rail particles leave the contact patch. Rather similar drawbacks are featured by the strip theory which, although giving a very good result regarding the shape of the contact area, fails to be accurate in predicting the tangential forces.

- Inside the contact ellipse, equation (1):

$$0 = \mathrm{w}_{\mathrm{x,y}} = \mathrm{V} \cdot \left(\nu_{\mathrm{x}} - \phi \cdot y,\ \nu_{\mathrm{y}} + \phi \cdot x \right) - V \frac{\partial u(x,y)}{\partial x} \tag{1}$$

- Outside the contact ellipse, equation (2):

$$0 = \mathrm{p}(\mathrm{x,y}) \tag{2}$$

Integrating Equation 1 it results, equation (3):

$$g(y) = \text{-}\mathrm{V} \cdot \mathrm{u}(\mathrm{x,y}) + V \left(\nu_x \cdot x - \phi \cdot x \cdot y,\ \nu_y \cdot x - \frac{1}{2} \phi \cdot x^2 \right) \tag{3}$$

where $g(y)$ is an arbitrary function.

The $g(y)$ arbitrary function should observe that the traction has to be continuous at the limit of the driving direction of the traction surface between the railway and the wheel. However, the result thus obtained presents a different limit value of the friction force than the rear limit of the contact force [6].

The traction increases up to the rear limit of the contact area where normal stress disappears and the traction drops to a null value. As a consequence, the friction's coefficient value has a discontinuous transition up to infinite.

The computation of the $g(y)$ expression gives a linear dependence between the forces and pseudo-sliding, equation (4):

$$\begin{aligned} F_x &= -a \cdot b \cdot G \cdot C_{11} \cdot \nu_x \\ F_y &= -a \cdot b \cdot G \left(C_{22} \cdot \nu_y + \sqrt{a \cdot b} \cdot C_{23} \cdot \phi \right) \\ M_\phi &= -\left(\sqrt[3]{a \cdot b} \cdot G \cdot C_{32} + (a \cdot b)^2 G \cdot C_{33} \cdot \phi \right) \end{aligned} \tag{4}$$

where: a, b – contact ellipse's semi-axes, ν_x, ν_y, φ - longitudinal, transversal and spin pseudo-sliding movements in the contact points, C_{11} , C_{22}, $C_{23,32}$, C_{33} – Kalker's coefficients which depend on the values of Poisson's coefficient and are being obtained based on the equations given below [7], equation (5):

$$C_{11} = -\frac{\partial F_x}{\partial \nu_x} / \left(a \cdot b \cdot G\right), \quad C_{22} = -\frac{\partial F_y}{\partial \nu_y} / \left(a \cdot b \cdot G\right)$$
$$C_{23} = -\frac{\partial F_y}{\partial \phi} / \left(\sqrt[3]{a \cdot b} \cdot G\right)_{\nu_x = \nu_y = \phi = 0} \tag{5}$$

Kalker is also defining the pseudo-sliding coefficients as following, [1], equation (6):

$$\kappa_x = \frac{a \cdot b \cdot G \cdot C_{11} \cdot \nu_x}{\mu \cdot N}, \quad \kappa_y = \frac{a \cdot b \cdot G \cdot C_{22} \cdot \nu_y}{\mu \cdot N}, \quad \kappa_\phi = \frac{\sqrt[3]{a \cdot b} \cdot G \cdot C23 \cdot \phi}{\mu \cdot N} \tag{6}$$

The longitudinal, transversal and spinning pseudo-sliding movement are determined based on the following relation, equation (7):

$$\nu_x = \frac{w_x}{V}, \quad \nu_y = \frac{w_y}{V}, \quad \phi = \frac{r \cdot \omega_s}{V}, \tag{7}$$

ω_s - the spinning angular speed. The $w_{x,y}$ pseudo-sliding speeds are established based on the (1).

3. Numerical application

The numerical application presented in this section takes into account an axle equipped with wheels featuring S78 profile (the nominal rolling radius is of 460 mm) on rails with profile type UIC 60, 1:20. The speed of the axle is of 35 m/s.

The value of the normal force applied on the wheel is 10 kN. In order to analyse the contact area, the wheel and rail profiles are described using circular arcs and the contact points are found through the method of the minimum distance [8, 9].

If two contact points occur on the same wheel, the normal load is distributed on the two contact patches. The ratios of the load on the two contact areas is determined assuming that the elasticity and force dependence on the deformations are the same for both of the points, according to Hertz [10] theory for the contact between two cylindrical bodies. Hence, the ratio of the vertical loads within the contact areas is given by equation (8):

$$Q_1 / Q_2 = \left(\delta_1 / \delta_2\right)^{3/2} \tag{8}$$

where δ_1 and δ_2 are the vertical projections of the penetrations in the two contact areas and the sum of the vertical projections of the normal loads in the contact areas, namely Q1 and Q2, balances the wheel load i.e, $Q_1 + Q_2 = Q$

In order to study wheel - rail tongue interaction an algorithm is developed within CONTACT software frame. The algorithm may take into account multiple contact points. The stages of the computation algorithm are as follows, [11], [12], [8]:

a. Coordinates for the first contact point are determined using the minimum height difference criteria.
b. Assuming that there is a single contact point, penetration is determined.
c. The possibility of an additional contact area is verified and the previous stages are iterated again, if necessary.
d. Final values of penetrations and normal loads are obtained.

Numerical studies of the axle operating conditions (i.e., traction or braking) upon penetrations and stresses in the wheel and turn out areas are described. Figures in the left column are for the rolling surface and in the right column for the flange surface.

Vector field of the tangential stress is represented in figures 1 - 4. Results in figures 1 and 2 are obtained considering that neither traction, nor braking is exerted by the axle, while in figures 3 and 4,

IOP Conf. Series: Materials Science and Engineering **400** (2018) 022057 doi:10.1088/1757-899X/400/2/022057

traction occurs. A stick area may be noticed on the rolling surface in the absence of traction, figure 1. The stick area disappears when traction occurs, figure 3, and the stress vector is augmented. Stress vector field remains rather similar on the flange in both situations, figures 2 and 4, and spin slip is not present in this area.

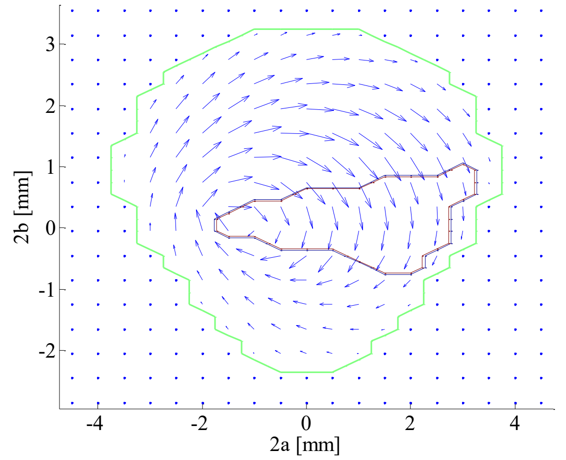

Figure 1. Stress vector field on the rolling surface area. No traction. Stick area is present.

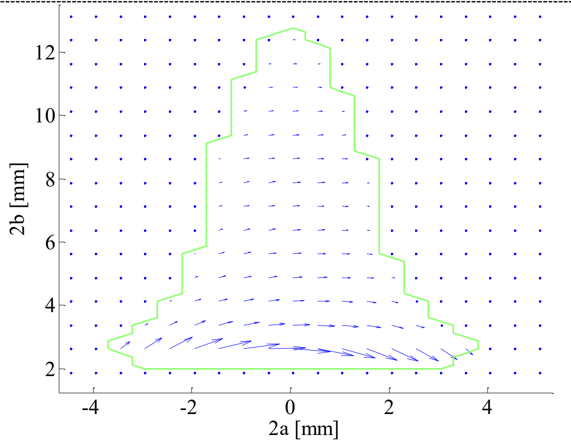

Figure 2. Stress vector field on the flange surface area. No traction. No spin slip.

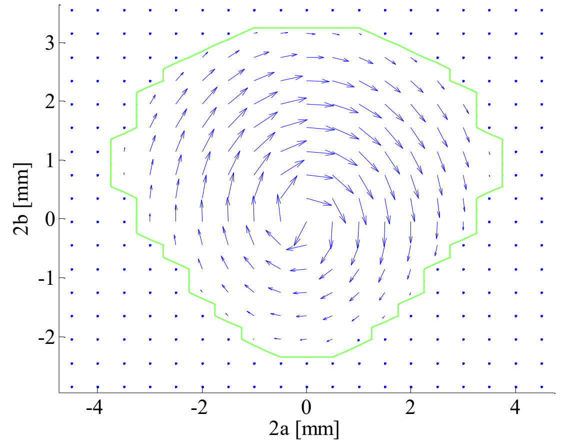

Figure 3. Stress vector field on rolling surface area. Traction occurs. Stick area disappeared. Stress vector field is augmented.

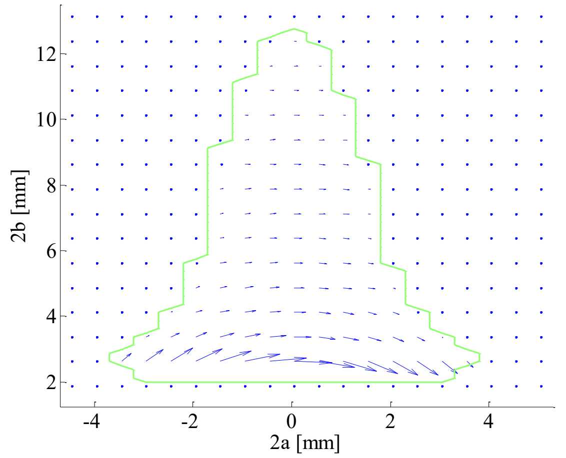

Figure 4. Stress vector field on the flange surface area. Traction occurs. No spin slip.

Friction power density is represented in figures 5-8. In accordance with the previous plots, the friction power density increases when traction increases. Figures 9-12 describe the distribution of the tangential stress in the wheel-turnout contact area.

According to figures 5-8, the friction power density is greater when the axle traction force occurs both on the rolling surface and the flange, figures 7 and 8, compared to the situation when the axle is braking. This fact is explained by the slip increase which aggravates wheel flange and inner turnout wear. At the same time, lateral axle displacements and slip are increased conducing to a negative influence upon the hunting movement.

IOP Conf. Series: Materials Science and Engineering **400** (2018) 022057 doi:10.1088/1757-899X/400/2/022057

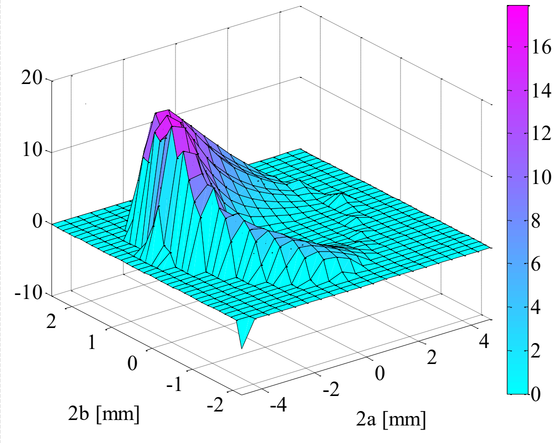

Figure 5. Friction power density for traction torque, on rolling surface area.

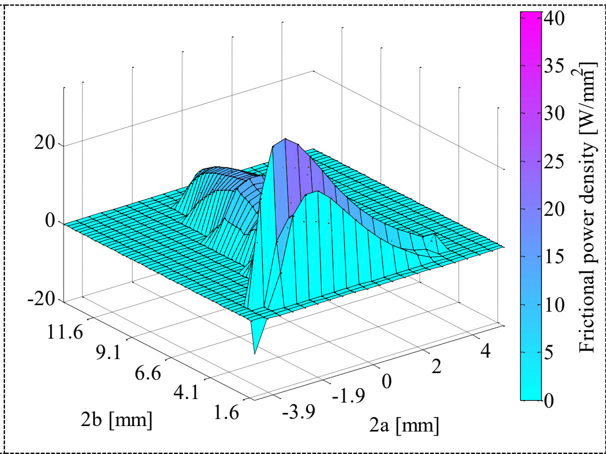

Figure 6. Friction power density for traction torque, on wheel flange area.

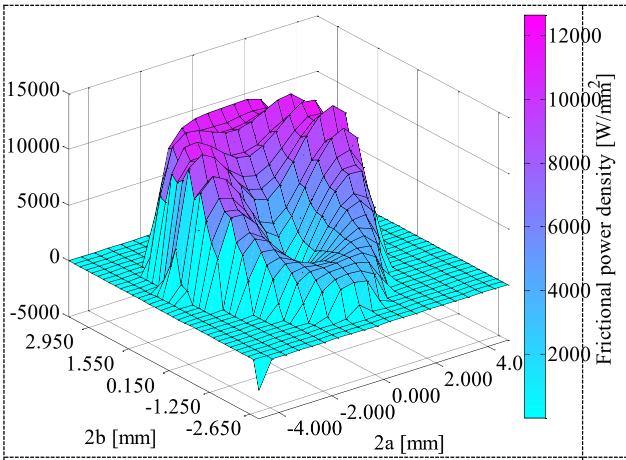

Figure 7. Friction power density for braking torque in the wheel-turnout contact area – wheel on rolling surface area.

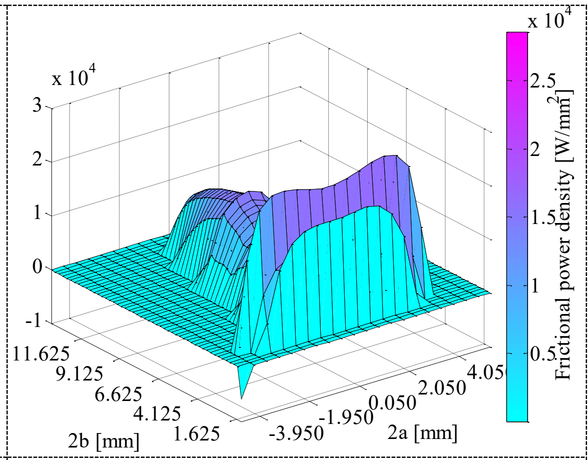

Figure 8. Friction power density for braking torque in the wheel-turnout contact area – wheel on wheel flange area.

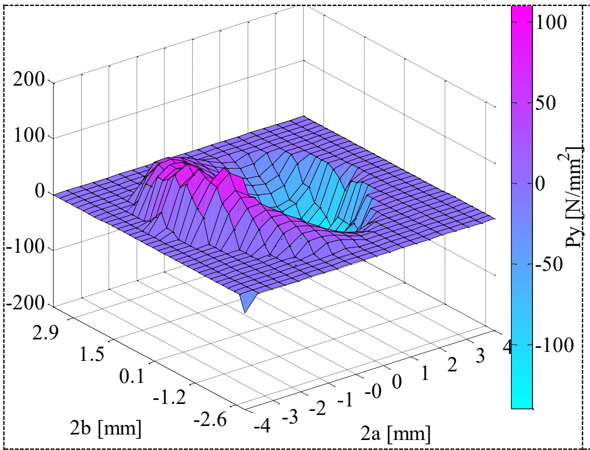

Figure 9. Distribution of the tangential stress for traction torque in the wheel-turnout contact area – wheel on rolling surface area.

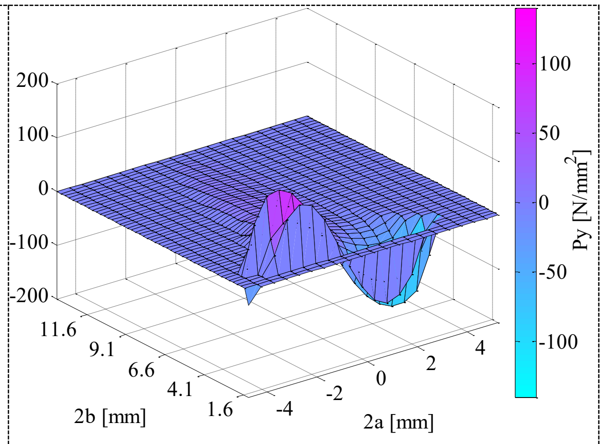

Figure 10. Distribution of the tangential stress for traction torque in the wheel-turnout contact area – wheel flange area.

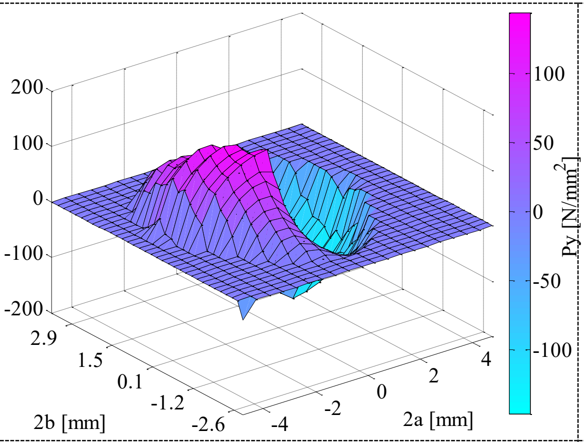

Figure 11. Distribution of the tangential stress for braking torque in the wheel-turnout contact area – wheel on rolling surface area.

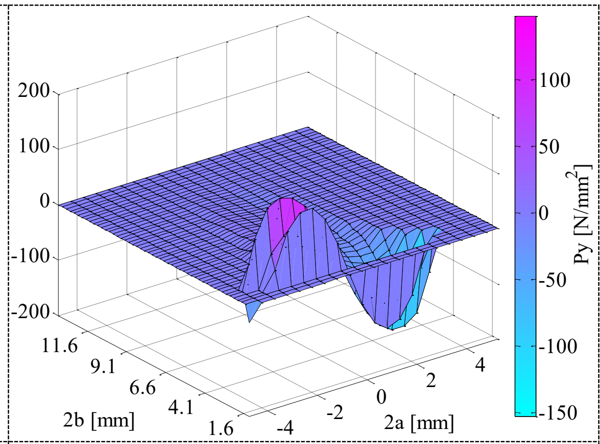

Figure 12. Distribution of the tangential stress for braking torque in the wheel-turnout contact area – wheel flange area.

The distribution of the tangential stress in the wheel-turnout contact area is plotted in figures 9 and 10 for traction torque and figures 11 and 12 for braking torque. In the wheel flange contact area, the tangential stress is significantly increased during traction mode due to the fact that guidance forces are also applied in this area, i.e., from 112 N/mm2 to 140 N/mm2, figure 9. In the wheel rolling surface area the variations are insignificant, i.e., from 140 N/mm2 to 142 N/mm2, figures 10-12.

The main parameter in the tangential forces expression is pseudo-sliding defined as the ratio between the sliding velocity in the contact point and the forward axle velocity. These parameters distinguish between static and rolling friction.

The present study brings a solution to obtain sliding velocities and stress distribution in the contact area which are essential for the study of the vehicle-rail interaction.

4. Conclusions

Wheel and turnouts life safe operation and life span prediction may be improved through a more thorough research. The approach proposed in this work is significantly more efficient from a numerical method point of view and it also allows computing the contact points position either on the fly or using look up tables. Numerical studies of the axle operating conditions (i.e., traction or braking) upon penetrations and stresses in the wheel and turn out areas are described.

Aspects of the influence of the axle operating conditions upon the wheel-turnout areas stresses are studied. In the wheel flange contact area, the tangential stress is significantly increased during traction mode while in the wheel rolling surface area the variations are insignificant. A wide class of problems may be solved using the present method.

5. References

[1] Sun Y Q, Cole C, McClanachan M 2010 The Calculation of Wheel Impact Force Due to the Interaction between Vehicle and a Turnout *Journal of Rail and Rapid Transit* **224** 391-403

[2] Kassa E, Andersson C and Nielsen J C O 2006 Simulation of dynamic interaction between train and railway turnout *Vehicle System Dynamics* **44** 247–258

[3] Gurule S and Wilson N 1999 Simulation of wheel/rail interaction in turnouts and special track work *Vehicle System Dynamics* **33** 143–154

[4] Kono H, Suda Y, Yamaguchi M, Yamashita H, Yanobu Y and Tsuda K 2005 Dynamic analysis of the vehicle running on turnout at high speed considering longitudinal variation of rail profiles *Proceedings of ASME International Design Engineering Technical Conferences and*

Computer and Information in Engineering Conference,5th International Conference on Multibody Systems, Nonlinear Dynamics and Control Parts **A, B,** and **C** 2149-2154

[5] Alfi S and Bruni S 2009 Mathematical modeling of train-turnout interaction *Vehicle System Dynamics* **47** 551–574

[6] Wiest M, Daves W, Nielsen J O C and Ossberger H 2008 Assessment of methods for calculating contact pressure in wheel-rail/switch contact *Wear* **265**(9-10) 1439–1445

[7] Kalker J J 1991 Wheel-rail rolling contact theory *Wear* **144** 243-261

[8] Sebeșan I and Tudorache C 2014 The contact between a wheel and a railway track and its influence on transportation safeness, *Scientific Bulletin - University Politehnica of Bucharest, Series D: Mechanical Engineering* **76**(3) 93-104

[9] Tudorache M C 2013 The influence of wheel-rail phenomena upon guiding safety for railway vehicle *PhD Thesis* Bucharest

[10] H Hertz 1882 Über die Berührung fester elastischerKörper *Journal Fur Die Reine Und Angewandte Mathematik* **92** 156-171

[11] Vollebregt E AH 2012 User guide for CONTACT Vollebregt & Kalker's rolling and sliding contact model *VORtech Computing the Scientific Software Engineers* 37-45

[12] Tudorache C and Oprea R 2015 A method for studying the interaction of wheel-turnout multi-point contact *Scientific Bulletin - University Politehnica of Bucharest, Series D: Mechanical Engineering* **77**(1) 37-50